separations

MDPI

Article

Composites Based on $CaCl_2$-$CaBr_2$ Salt System for Adsorption Applications: Designing the Optimal Sorbent for Gas Drying and Air Conditioning

Alexandra Grekova [1,*], Marina Solovyeva [1], Anastasiia Cherpakova [1,2] and Mikhail Tokarev [1]

[1] Boreskov Institute of Catalysis, Lavrentiev Avenue. 5, Novosibirsk 630090, Russia; solovyeva@catalysis.ru (M.S.); tokarev@catalysis.ru (M.T.)
[2] Department of Natural Sciences, Novosibirsk State University, Pirogova Str. 2, Novosibirsk 630090, Russia
* Correspondence: grekova@catalysis.ru

Abstract: The different adsorption applications require the development of sorbents with predetermined properties. One of the ways for fine tuning the adsorption properties of the material is using a binary salt system as an active sorbing component. The aim of this work is to conduct a precision investigation of thermodynamic data on the sorption equilibrium of composite sorbents "($CaCl_2$ + $CaBr_2$) confined to the silica gel pores" with water vapour. The isotherms and isosteres (at an uptake of N = 1.5 and 3.6 mole/mole) of water sorption on the composites were measured. It was shown that at a fixed temperature, the composites based on solid solutions of $CaCl_2$ in $CaBr_2$ form complexes with water at a pressure that is dependent on the $CaCl_2$/$CaBr_2$ molar ratio. The isosteric enthalpy and entropy of water sorption ($\Delta H = -48 \pm 3$ kJ/mol $\Delta S = -108 \pm 2$ J/(mol·K)) at N = 3.6 mole/mole were midway between the same parameters for composites on the base of the pure salts $CaCl_2$ and $CaBr_2$. The novelty of this work is in the design of sorbents optimized for air conditioning in hot climates and air drying cycles. It was shown that the use of the binary $CaCl_2$ + $CaBr_2$ system confined to the silica pores can be an effective tool for designing innovative materials with predetermined properties.

Keywords: water adsorption; calcium halides; porous materials; predetermined properties; air conditioning; dehumidification

Citation: Grekova, A.; Solovyeva, M.; Cherpakova, A.; Tokarev, M. Composites Based on $CaCl_2$-$CaBr_2$ Salt System for Adsorption Applications: Designing the Optimal Sorbent for Gas Drying and Air Conditioning. *Separations* **2023**, *10*, 473. https://doi.org/10.3390/separations10090473

Academic Editor: Xinhua Qi

Received: 2 August 2023
Revised: 24 August 2023
Accepted: 25 August 2023
Published: 28 August 2023

1. Introduction

Adsorption is widely used in numerous applications, among which are the purification, separation and storage of gases, maintaining relative humidity, adsorptive cooling, heat storage, etc. [1]. The phenomenon of adsorption is based on the sorption of vapours by the surface of a porous media (adsorbent). In industry, sorbents such as silica gels, zeolites and activated carbons are widely used. Unfortunately, such widespread adsorbents are not always the most optimal for a specific practical application. Indeed, the requirements of various applications of the adsorbent can differ significantly since the processes' efficiency is extremely sensitive to the sorption equilibrium in the "adsorbent—working fluid" pair [2–4].

An ideal adsorbent for gas drying will not be suitable for maintaining humidity at a given value of relative pressure (Figure 1a). Moreover, the requirements for the adsorbent can differ significantly even within the same practical application, depending on the conditions in which the device will operate. For example, let us consider two air conditioning adsorption cycles with the same cooling temperature of 5 °C but under different climatic conditions (Figure 1b): (1) standard air conditioning—ambient temperature 35 °C, regeneration temperature 80 °C and (2) air conditioning for a very hot climate with an ambient temperature of 45 °C and regeneration temperature of 100 °C. Polanyi boundary potentials ΔF [5] calculated for given climate data clearly demonstrate that a

sorbent capable of exchanging a large amount of working fluid in the first "cycle window" exchanges almost nothing in the "cycle window" for hotter climates, and vice versa. In other words, the improvement of adsorptive processes is closely connected with the development of new adsorbents with predetermined properties. However, despite the wide variety in the requirements imposed by different applications on the desirable adsorbent properties, only a few types of porous adsorbents are used in actual practice—silica gels, alumina, zeolites and porous carbons [6–8]. Varying the chemical nature and porous structure of these single-component adsorbents is the main possibility for the alteration of their adsorption properties. The surface modification of common adsorbents with the use of various functional groups is an alternative way to affect their adsorption properties, which gives diverse hybrid "organic-inorganic" and composite adsorbents [9]. Indeed, through physico-chemical treatment, the moisture adsorption properties of materials can be changed [10,11].

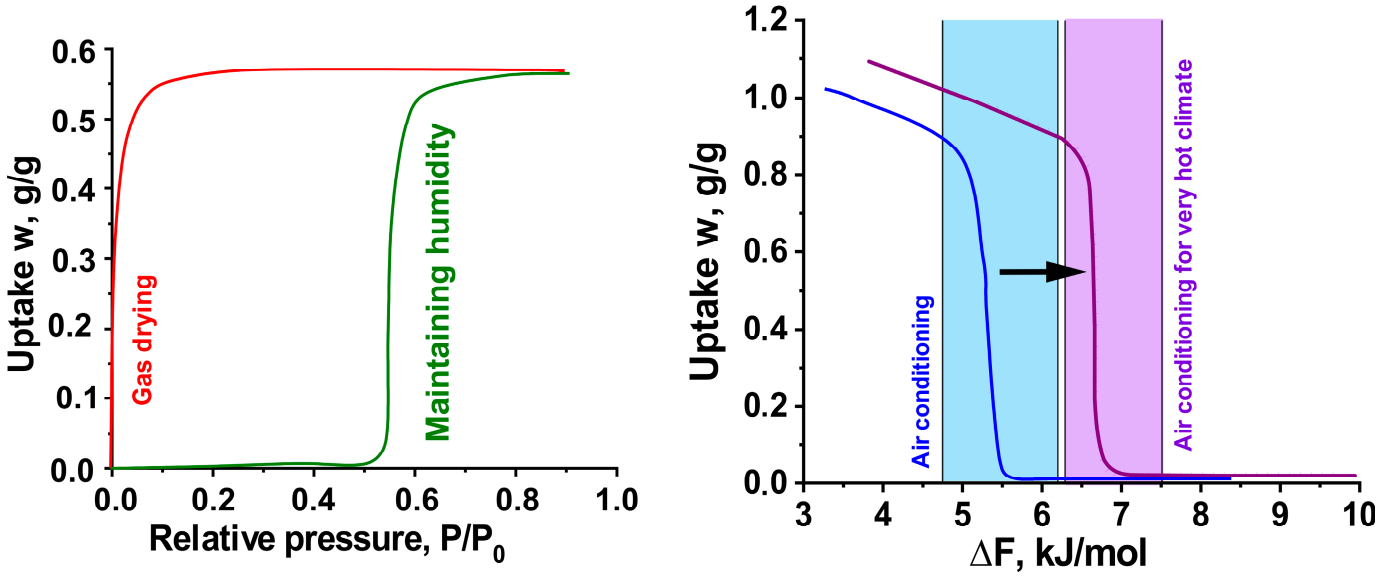

Figure 1. (**a**) Optimal adsorbent for gas drying (red line) and maintaining humidity (green line); (**b**) boundary potentials for typical air conditioning cycle (blue area) and air conditioning cycle for extremely hot climate (violet area).

The present-day level of material science allows *a target-oriented design of novel porous materials adapted to a particular application*. Indeed, very often, composite materials demonstrate more impressive results than nonmodified traditional sorbents. The modified sorbents demonstrate affinity to both organic [12–14] and inorganic [15,16] compounds/pollutants. The composites materials "Salt inside a porous matrix" (CSPM) are characterised by a high sorption ability (0.4–1.4 g/g) caused by the reaction of salt confined into matrix pores with water, methanol or ammonia [17–19]. The sorption properties of CSPMs can be intently designed by variations in the composite's components and parameters of synthesis [20–22]: (1) the chemical nature of active salt and the host matrix [20,23,24], (2) the matrixes' porous structure [21,25], (3) the salt content [22], (4) the pH of the impregnating solution [20] and (5) the temperature of the composite drying [20].

A number of studies have considered tailoring the sorbent properties in accordance with the requirements of the particular application by embedding two salts into matrix pores [26–28]. In [27], it was shown that by partially substituting $MgSO_4$ by $MgCl_2$, the relative humidity over the mixture was changed. The phenomenon of changing the properties of solid solutions compared to the properties of the individual components is now well known [29]. It has been shown that during the formation of a solid solution,

the parameters of crystal lattices change monotonically. In the first approximation, this dependence of the parameter on the content of the dissolved component is linear and is known as the Vegard rule [30]. The change in the crystal lattice parameter during the formation of a solid solution also leads to a change in its physico-chemical properties.

This phenomenon has been used to reduce the melting temperature of $CaCl_2 \cdot 6H_2O$ hexahydrate in heat storage systems [31]. The use of the $CaBr_2 \cdot 6H_2O$ additive makes it possible to decrease the melting point of $CaCl_2 \cdot 6H_2O$ from 30 °C to 16 °C, while the addition of nonisomorphic KCl reduces the melting temperature of the system insignificantly. The addition of calcium bromide gives a greater effect on the thermodynamic characteristics of the system than the addition of potassium chloride since the $CaCl_2$-$CaBr_2$ system forms a homogeneous solid solution over the entire concentration range [32]. To change the formation temperature of calcium halide ammoniates for ammonia storage systems, it is proposed to use solid solutions $CaCl_2$-$CaBr_2$ [33,34]. The authors studied ammonia sorption by a series of systems with different molar ratios of salts: $CaCl_2$, $CaCl_{1.67}Br_{0.33}$, $CaCl_{1.33}Br_{0.67}$, CaClBr, $CaCl_{0.67}Br_{1.33}$, $CaCl_{0.33}Br_{1.67}$ and $CaBr_2$, and it was shown that the pressure at which the sorption process begins decreases with increasing calcium bromide concentration in the system (28.7, 14.1, 5.2, 3.2 and 1.2 kPa, respectively). Thus, the reaction of the formation of ammoniates for a solid solution of calcium halides occurs at a temperature midway between the temperatures at which the formation of the ammoniates of individual salts takes place. The authors explain this effect by changing the electric potential of the cation when it is surrounded by different anions [34]. Apparently, this is of decisive importance since it is to the cation that the molecules of the sorbed substance (ammonia, water or alcohol) are coordinated. It is also important to note that in the case of solid solution formation, the characteristic sorption curve (sorption isotherm) of ammonia is not a linear combination of the sorption curves of individual components.

During the formation of a solid solution of salts, it becomes possible to vary the sorption characteristics of the system. The effect of changing the reaction temperature can be used to "tune the properties" of the system to the requirements of the process in which it is used. For a system based on a binary salt system $BaCl_2$-$BaBr_2$, a series of studies was carried out, and at first, the fundamental possibility of shifting the sorption equilibrium was shown due to the formation of a solid solution of salts in the pores of the matrix (silica gel [35] and expanded vermiculite [36])—the position of the step on the isobars corresponding to the chemical reaction between salt and ammonia shifted towards high temperatures with an increase in the concentration of barium bromide in the composite. Then, taking into account the change in the sorption equilibrium during the formation of a solid solution in the matrix pores, composites specialized for applications of adsorption cooling [37] and ice making [38] were synthesized. It was shown that the synthesized materials do indeed meet the initially specified requirements. However, for sorbtives such as water and alcohols, only the principal possibility of shifting the equilibrium [35,39] by the formation of a salts' solid solution ($CaCl_2$-$CaBr_2$; LiCl-LiBr) inside the pores of the matrix was previously shown, without specifying for which applications this effect could be used.

The purpose of this work is to study in detail the thermodynamic parameters (enthalpy and entropy) of water sorption on the composites based on the $CaCl_2$-$CaBr_2$ binary salt system. Thermodynamic parameters of the sorption equilibrium for such a system are important both from fundamental and chemical engineering points of view. In order to achieve the stated aim of the work, the following tasks were solved: (1) sorbents with different molar salt contents were synthesized, (2) for the synthesized composites, the sorption equilibrium with water vapour was studied by the volumetric method, (3) based on sorption data, the effect of the composition of the samples on their sorption properties was analysed, and (4) recommendations are given on the composition of the optimal sorbent for two practical applications (air conditioning in hot climates and air drying). A flowchart of the study is presented in Figure 2.

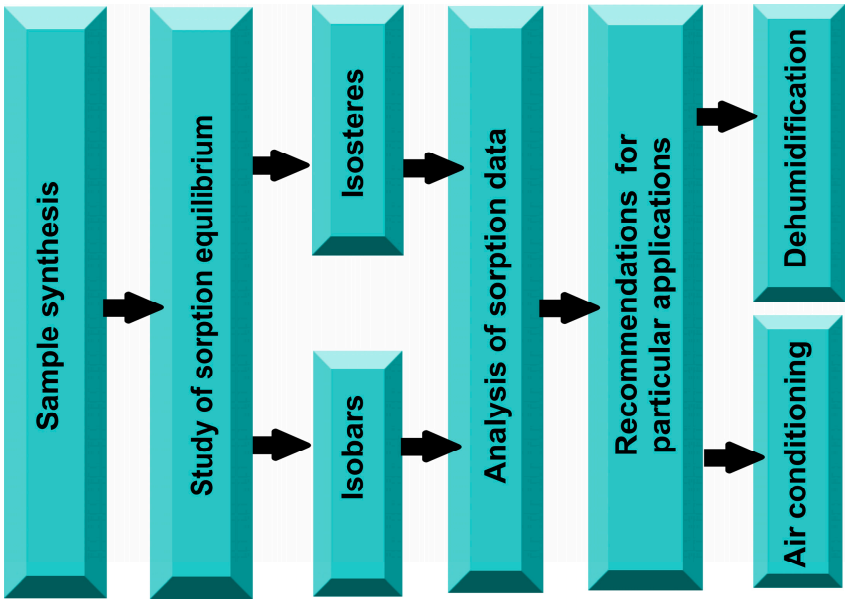

Figure 2. The research methodology.

2. Materials and Methods

2.1. Materials and Synthesis

Commercial silica gel Davisil Gr. 646 (the average pore diameter d_{av} =15 nm (BET), the specific surface area S_{sp} = 300 m^2/g (BET), the pore volume V_p = 1.18 cm^3/g) was used as a host matrix. Calcium chloride and bromide were purchased from Aldrich and used as delivered. The mixed $CaCl_2$ + $CaBr_2$ aqueous solutions were prepared with different molar ratio $CaCl_2/CaBr_2$ = 1:0, 3:1, 1:1, 0:1. The composites were synthesized by an "incipient wetness" impregnation method. The silica gel was dried at 160 °C for two hours, impregnated with an appropriate amount of mixed salts solution and dried again at 160 °C until the sample weight became constant. A number of composites ($CaCl_2$ + $CaBr_2$)/SiO_2 were synthesized; the molar content of calcium in all the samples equals L_{Ca} = 2 mmole per 1 g of the composite. The samples were designated as $CaCl_2/SiO_2$, ($CaCl_2$ + $CaBr_2$ (3:1))/SiO_2, ($CaCl_2$ + $CaBr_2$ (1:1))/SiO_2, ($CaCl_2$ + $CaBr_2$ (3:1))/SiO_2 and $CaBr_2/SiO_2$ (Table 1).

Table 1. The composition of the sorbents ($CaCl_2$ + $CaBr_2$)/SiO_2, C_{CaCl2}, C_{CaBr2}, C_{SiO2}—the weight content of $CaCl_2$, $CaBr_2$ and SiO_2, respectively.

Sample	Mole $CaCl_2$/Mole $CaBr_2$	C_{CaCl2}, wt %	C_{CaBr2}, wt %	C_{SiO2}, wt %
$CaBr_2/SiO_2$	0/1	0	41	59
($CaCl_2$ + $CaBr_2$ (1:1))/SiO_2	1/1	11	21	68
($CaCl_2$ + $CaBr_2$ (3:1))/SiO_2	3/1	17	10	73
$CaCl_2/SiO_2$	1/0	23	0	77

2.2. Sorption Isotherms' Measurement

The isotherms of water sorption on the composites were measured by a standard volumetric method at a constant temperature T = 65 °C. The main parts of the experimental rig (Figure 3a) are the adsorber (volume V_{ad} = 174 mL, Figure 3b), the buffer tank (volume V_b = 28.436 L), the evaporator, and the system of connecting pipes and taps. All of these parts were placed in a thermally insulated box maintained at T = 35 °C in order to avoid condensation. To keep the adsorber temperature constant, a liquid thermostat Julabo F25 was used. The temperatures were measured using a K-type thermocouple with an accuracy of ±0.2 °C. In order to collect experimental data, the analog-to-digital converter ADAM4019 was used.

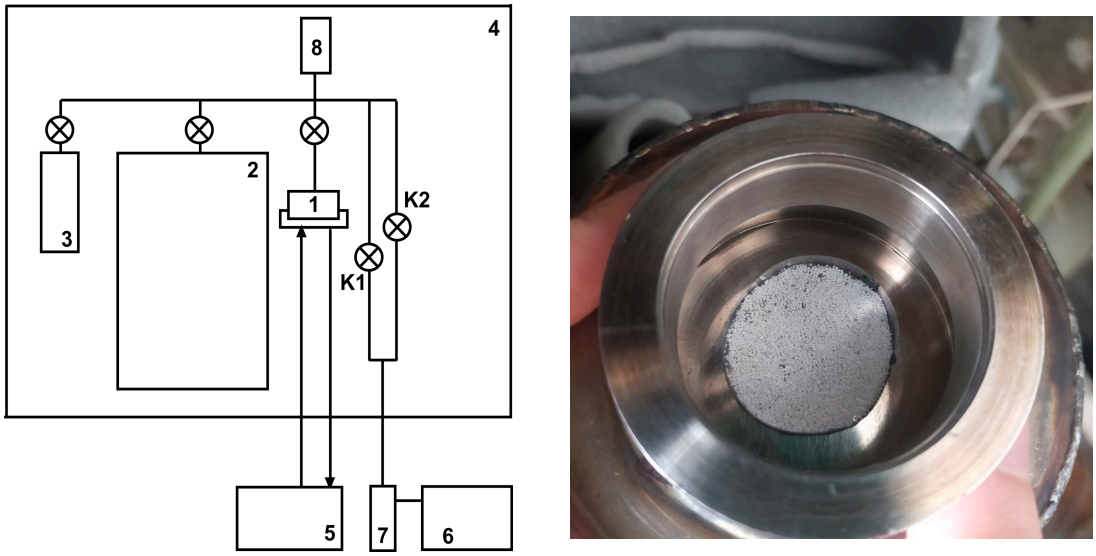

Figure 3. (**a**) Schematic diagram of the installation for measuring the water sorption isotherms: 1—adsorber, 2—buffer tank, 3—evaporator, 4—heating box, 5—thermostat, 6—vacuum pump, 7—nitrogen trap, 8—digital pressure gauge, K1—needle valve, K2—ball valve.; (**b**) photo of adsorber.

The sample (300–500 mg), previously dried at 160 °C, was placed in the adsorber, and evacuated at 90 °C for two hours in order to remove residual water adsorbed on the composite. For system evacuation, a vacuum pump with a nitrogen trap was used. In order to prevent the sample from blowing out of the adsorber at the beginning of the evacuation, an Edwards LV10K needle valve K_1 was used. After the pressure was reduced to 3–4 mbar, the ball valve K_2 (Edwards IBV16MKS) was opened. Then the sample was cooled down to a fixed temperature, and after that the sample was cooled to 65 °C using a liquid thermostat. The water in the evaporator was subjected to double degassing. The interval between the first and second stages of degassing was about 12 h. Before the start of the experiment, water vapours were let into the previously evacuated buffer volume. The change in the pressure in the system was determined using a digital pressure gauge (Baratron 622D) with an accuracy of ±(0.1–0.3) mbar depending on the measured value.

After establishing a constant pressure P_1 in the buffer tank, the latter was connected to the adsorber. This caused a pressure drop in the system to the value of P_2, due to both gas expansion and the sorption process. The system was kept until the equilibrium was reached for 3–20 h. The value of the pressure drop due to gas expansion P_{ex} was calculated from the mass balance when the gas was passed from the buffer tank to the adsorber without a sorbent. The sorption uptake was calculated as the equilibrium number of sorbed moles related to one Ca^{2+} mole $N(P,T) = [m(P,T)/M]/(m_{ad}L_{Ca})$ where M is a molar weight of H_2O and L_{Ca} is the molar content of calcium. The accuracy of the adsorption measurements was $\Delta N = \pm 0.06$ mole H_2O/mole Ca^{2+}.

2.3. Sorption Isosteres' Measurement

The sorption equilibrium of the composites with water vapour was studied by the isosteric sorption method [40]. The isosteres are lines of constancy of the composition of the "composite—sorbed substance" system [23,41,42]. In other words, with a simultaneous change in the temperature of the sorbent and the vapour pressure of the liquid above it, it is possible to maintain a constant amount of liquid absorbed by the sorbent. Thus, in the case of air conditioning cycles, the sorbent's regeneration stage and obtaining cold are isobaric, whereas the intermediate stages are isosteric [43]. Indeed, at this moment, the sorbent is disconnected from the evaporator and condenser; therefore, despite the change

in the temperature of the sorbent, the amount of absorbed substance does not change. The isosteres of water were measured at temperature ranges T = 60–135 °C; the pressure ranges were P(H_2O) = 4–135 mbar. The main components of the experimental rig are an adsorber (110 ± 0.1 mL) filled with composite, an evaporator, a pressure gauge (Setra 769), pipes, a system of valves (Edwards IBV16MKS, Edwards LV10K needle valve) and a vacuum pump (Edwards RV8) (Figure 4). It is important to note that the volume of pipes ("Dead volume" of the setup) should be minimized because a decrease in the dead volume results in an increase in measurement accuracy. Indeed, if the pipes' volume is properly minimized, the ratio between the amount of water in a gaseous state and in an adsorbed state is minimized too.

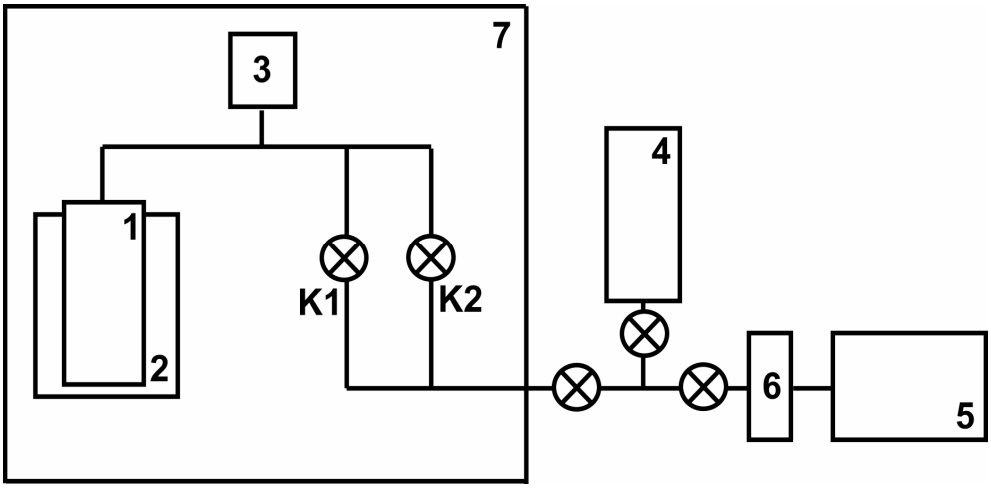

Figure 4. The scheme of experimental setup for measuring the isosteres of water sorption: 1—adsorber, 2—electric oven, 3—pressure gauge, 4—evaporator, 5—heat pump, 6—nitrogen trap, 7—heating box, K1—needle valve, K2—ball valve.

The composite sorbent of the dry weight m_{ad} = 50.0 ± 0.1 g was placed inside the adsorber, evacuated for 2 h to the residual pressure 0.1 mbar at 90 °C and cooled down to an ambient temperature (Julabo F25). The adsorber was connected with the evaporator and the sample was saturated with a certain amount of sorbtive up to fixed uptake N. Then the measuring cell was disconnected from the evaporator and kept for 12 h to reach uniform sorbate distribution inside the adsorber. Then the adsorber temperature was increased to a fixed value that resulted in the rise of the pressure over the adsorbent. The pressure and temperature were monitored continuously until the equilibrium was reached and the pressure P = f(T) was registered. The criterion for the equilibrium was constant pressure (±0.1 mbar) in the system for 2 h. During the measurements under increasing temperatures, some amount of the sorptive desorbed from the sample into the empty volume of the apparatus (the "dead volume"). As the temperature increases, the change in the content of the water is 0.05 mol/mol salt, respectively. Thus, the water content in the sorbent can be considered constant within the specified accuracy.

The plotting of experimental data in the Clausius–Clapeyron coordinates makes it possible to determine the values of the enthalpy and entropy of sorption depending on the content of the water in the sorbent in accordance with the equation:

$$\ln(P) = A + B/T \quad (1)$$

where A = −ΔS/R, B = ΔH/R (ΔS—isosteric entropy of sorption, ΔH—isosteric enthalpy of sorption, R—universal gas constant). The accuracy of measuring the heat of sorption was ±3 kJ/mol, and the accuracy of entropy was ±3 J/(mol·K).

3. Results

There are three steps in the sorption isotherm of $CaBr_2/SiO_2$ (Figure 5). The first step takes place in the pressure range P = 0–0.5 mbar and corresponds to the formation of monohydrate $CaBr_2 \cdot H_2O$. With a further increase in pressure, the monohydrate reacts with one more water molecule at P = 1.5–3 mbar, forming the di-hydrate in accordance with the reaction $CaBr_2 + 2H_2O = CaBr_2 \cdot 2H_2O$. Then the di-hydrate reacts with two more water molecules, forming tetrahydrate $CaBr_2 \cdot 2H_2O + 2H_2O = CaBr_2 \cdot 4H_2O$. The further pressure rise results in a gradual increase in sorption at P > 11 mbar. Such behaviour corresponds to the formation of the salts' water solution inside the matrix pore.

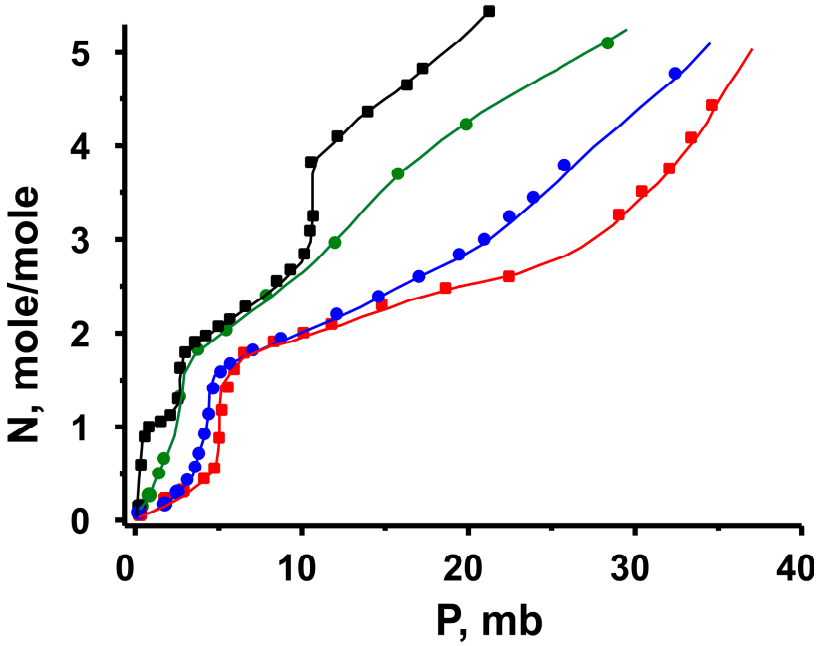

Figure 5. The isotherms of water sorption on the composites $(CaCl_2 + CaBr_2)/SiO_2$: (■)—$CaBr_2/SiO_2$, (●)—$(CaCl_2 + CaBr_2$ (1:1))$/SiO_2$, (●)—$(CaCl_2 + CaBr_2$ (3:1))$/SiO_2$, (■)—$CaCl_2/SiO_2$ obtained at T = 65 °C.

Due to the lower affinity of $CaCl_2$ to water, the sorption isotherm for the $CaCl_2/SiO_2$ composite is shifted towards a higher pressure with regards to that for $CaBr_2/SiO_2$. For the isotherm of water sorption by the composite based on $CaCl_2$, one can observe a step corresponding to the reaction $CaCl_2 + 2H_2O = CaCl_2 \cdot 2H_2O$ at P = 5–7 mbar followed by a plateau with N ≈ 2 mol/mol and a further rise in uptake at P ≥ 20 mbar.

The isotherms of water sorption on the binary salt composites $(CaCl_2 + CaBr_2$ (1:1))$/SiO_2$ and $(CaCl_2 + CaBr_2$ (3:1))$/SiO_2$ (Figure 5) are located between the isotherms of composites based on the single salts. For the composite $(CaCl_2 + CaBr_2$ (3:1))$/SiO_2$ (blue), the transition corresponding to the reaction $CaCl_xBr_{2-x} + 2H_2O = CaCl_xBr_{2-x} \cdot 2H_2O$ is slightly shifted towards a lower pressure ΔP = 1 mbar relative to the same transition for the sample $CaCl_2/SiO_2$. At higher uptakes N = 2–4 mole/mole, a shift in pressure achieves 5–6 mbar. For the sample $(CaCl_2 + CaBr_2$ (1:1))$/SiO_2$ (green), there is a change in the equilibrium pressure of the monohydrate formation by the transition $CaCl_xBr_{2-x} + H_2O = CaCl_xBr_{2-x} \cdot H_2O$, relative to the corresponding pressure for $CaBr_2/SiO_2$. This transition is shifted towards higher pressures by ΔP = 0–2 mbar. It is interesting to note that the sorption isotherms of composites $(CaCl_2 + CaBr_2$ (1:1))/SiO and $CaBr_2/SiO_2$ are virtually identical in the pressure range $2 \leq P \leq 8$ mbar where N = 1.5–2.5 mol/mol. The transition corresponding to the formation of a solution is shifted to higher pressures with ΔP = 6–7 mbar.

The probable explanation of the abovementioned change in the equilibrium pressure of reactions is the formation of the solid solution of calcium halides inside silica gel pores. Indeed, the dissolution of $CaBr_2$ in the crystalline lattice of $CaCl_2$ results in the broadening

of the spacing parameter that probably promotes the incorporation of water molecules in the lattice and the decrease in the equilibrium pressure of the solvate formation from the salt.

From the isosteres of water sorption on composites $CaBr_2/SiO_2$, ($CaCl_2$ + $CaBr_2$ (1:1))/SiO_2 and $CaCl_2/SiO_2$ at uptakes N = 1.5, 3.6 ± 0.05 mole/mole (Figure 6), the isosteric entropy and enthalpy of sorption were found (Table 2).

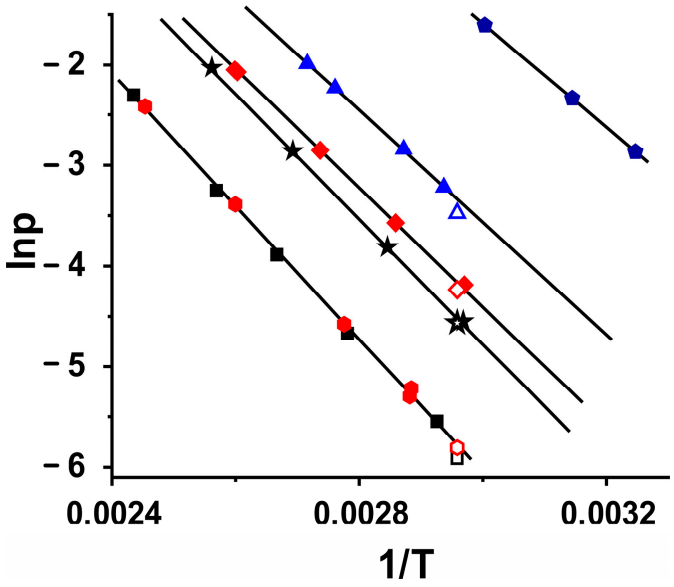

Figure 6. Isosteres of water sorption on composites ($CaCl_2$ + $CaBr_2$)/SiO_2: N = 3.6 ± 0.05 mole/mole (▲, △)—$CaCl_2/SiO_2$, (◆, ◇)—($CaCl_2$ + $CaBr_2$ (1:1))/SiO_2, (★, ☆)—$CaBr_2/SiO_2$; N = 1.5 ± 0.05 mole/mole (■, □)—$CaBr_2/SiO_2$, (⬢, ⬡)—($CaCl_2$ + $CaBr_2$ (1:1))/SiO_2; ⬟—water liquid–gas equilibrium line. Open symbols—data obtained by measuring the sorption isotherms.

Table 2. The enthalpy and entropy of water sorption on ($CaCl_2$ + $CaBr_2$)/SiO_2 composites at N = 1.5, 3.6 ± 0.05 mole/mole.

Sample	N, Mole/Mole ± 0.05	ΔH, kJ/Mole	ΔS, J/(Mole·K)
$CaBr_2/SiO_2$	3.6	−51 ± 3	−115 ± 3
$CaCl_xBr_{2-x}/SiO_2$-1:1	3.6	−48 ± 3	−108 ± 3
$CaCl_2/SiO_2$	3.6	−46 ± 3	−109 ± 3
$CaBr_2/SiO_2$	1.5	−55 ± 3	−114 ± 3
$CaCl_xBr_{2-x}/SiO_2$-1:1	1.5	−55 ± 3	−115 ± 3

In the case of the water content in the samples, N = 3.6 ± 0.05 mole/mole, the isosteric enthalpies for samples $CaBr_2/SiO_2$, ($CaCl_2$ + $CaBr_2$ (1:1))/SiO_2 and $CaCl_2/SiO_2$ are close to each other. However, there is a trend of the increasing modulus of the enthalpy of the sorption with an increasing $CaBr_2$ content in the sample. The water sorption entropy also increases with the increase in the $CaBr_2$ content in the composite. For water content N = 1.5 mole/mole, the thermodynamic parameters (Table 2) of the sorption equilibrium for composites $CaBr_2/SiO_2$ and ($CaCl_2$ + $CaBr_2$ (1:1))/SiO_2 are very close, which is consistent with the water sorption isotherms of the abovementioned composites in the pressure range $2 \leq P \leq 8$ mbar (Figure 5). The enthalpy and entropy obtained for N = 1.5 mole/mole are higher than those for N = 3.6 mole/mole. This fact is consistent with the published data [44] for $CaCl_2/SiO_2$—the water system. It was shown that an increase in N from 1 to 10 results in a decrease in the heat of sorption from 63.1 to 43.9 kJ/mol. This phenomenon can be explained by the fact that the first portions of water tend to occupy the most energetically favourable sites, and as a result, the higher heat of sorption is observed. It is worth

noting that the data from isosteric experiments agree well with the data obtained by the measurement of sorption isotherms (Figure 5).

The observed shift in the solvate formation positions with the change in the $CaCl_2/CaBr_2$ ratio illustrates that the use of the binary salt system to form solid solutions can be an effective tool to manage the sorption properties of the composites "salt inside porous matrix" in order to meet the requirements of particular applications.

4. Discussion

As was shown above, by varying the ratio of salts in the pores of the matrix one can purposefully change the thermodynamic characteristics of the sorption equilibrium of the system "working fluid—sorbent". Let us consider the prospects of this conception for designing the optimal sorbent for air conditioning and dehumidification applications.

4.1. Air Conditioning for Hot Climate

The air conditioning adsorption cycle [43] is determined by three temperatures (Figure 6): (1) the target refrigeration temperature (evaporator temperature T_{ev}), (2) the ambient temperature (condenser temperature T_{con}), and (3) the regeneration temperature (T_{reg}). Usually, the typical adsorption air conditioning cycle considered in the literature operates at an ambient temperature T_{con} = 30–35 °C [43,45]. As was shown in the Introduction (Figure 1b), in the case of a hotter climate (T_{con} = 45 °C), the use of an adsorbent specialized for these conditions is required. In this work, the cycle of adsorption air conditioning in a hot climate (T_{ev} = 5 °C, T_{con} = 45 °C, T_{reg} = 110 °C) was considered. To assess the prospects of various working pairs under cycle conditions, it is necessary to calculate the Polanyi boundary potentials for the stages of adsorption (3–4 Figure 7a) and desorption (1–2, Figure 7a):

$$\Delta F_a = -RT_{con} \ln\left(P_{ev}/P^0(T_{con})\right), \quad (2)$$

where $P^0(T_{con})$—saturated pressure of working fluid at temperature T_{con}.

$$\Delta F_d = -RT_{reg} \ln\left(P_{con}/P^0(T_{reg})\right) \quad (3)$$

where $P^0(T_{reg})$—saturated pressure of working fluid at temperature T_{reg}.

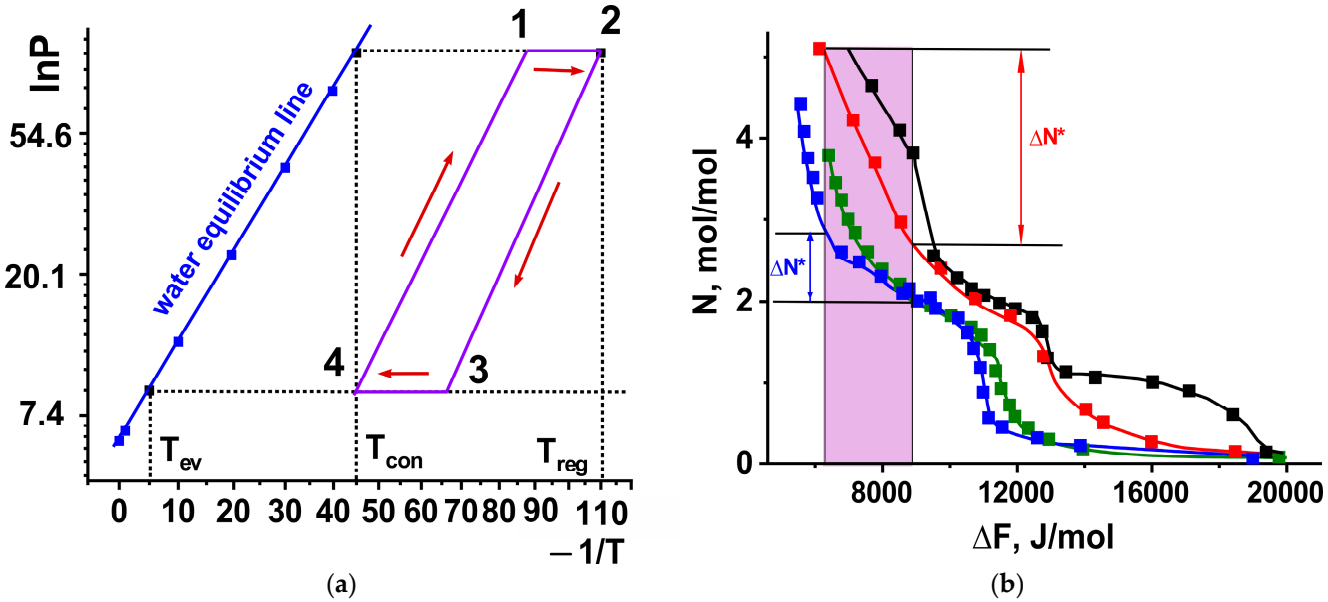

Figure 7. (**a**) Air conditioning adsorption cycle; (**b**) dependence "N vs. ΔF" (■)—$CaCl_2/SiO_2$, (■)—($CaCl_2$ + $CaBr_2$(3:1))/SiO_2, (■)—($CaCl_2$ + $CaBr_2$(1:1))/SiO_2, (■)—$CaBr_2/SiO_2$, pink area—window of cycle. Arrows show the consequence of the stages.

Boundary values of the Polanyi potential ΔF_a = 6.3 kJ/mol and ΔF_d = 8.9 kJ/mol form a window of the cycle (pink area Figure 7b). The composite based on single salt $CaCl_2$ can be used at T_{con} = 30–35 °C [46]. However, from the experimental data (Figure 7b) it is clear that at T_{con} = 45 °C this composite demonstrates the lowest uptake change (ΔN*-blue) among the tested materials. It can be seen that in the given range of adsorption potential values, the composite sorbent with a salt ratio of 1:1 exchanges the largest amount of water (ΔN*-red).

It is important to note that it is known in the literature that widespread working pairs allow a cooling effect of 10–17 °C to be reached at an ambient temperature of about 30 °C. However, the proposed material can be used in a much hotter climate (at an ambient temperature of 45 °C) and provides a cooling effect of 5 °C (Table 3).

Table 3. Literature data on working pairs and cycles' condition for adsorption chilling.

Working Pair	Cooling Temperature T_{ev}, °C	Ambient Temperature T_{con}, °C	Regeneration Temperature T_{reg}, °C	Reference
Silica gel/water	17	30	85	[47]
SAPO34-water	9	30	130	[48]
SAPO34-water	7	30	82	[49]
Zeolite 13X/$CaCl_2$)/water	14	31	85	[50]
Zeolite (SAPO-34)/water	10	30	85	[51]
Silica gel RD-2060; zeolite AQSOA-Z02	10	30	95	[52]
Zeolite 13X/$CaCl_2$ − water	14	28	85	[53]
activated carbon-methanol	5	30	100	[54]

The bulk density of such a sorbent is 0.53 g/cm^3. Knowing the bulk density of the material, it is possible to estimate how much sorbent can be loaded into the adsorber heat exchanger. Paper [55] discusses the possibility of optimizing the geometry of a finned flat tube (FFT) heat exchanger (Figure 8) for the application of adsorption cooling by varying the distance between the primary and secondary heat-removing elements. A real heat exchanger with a geometry close to the optimal geometry calculated in [55] is presented in [56]. Let us estimate the amount of sorbent based on a binary salt system that can be loaded into such a heat exchanger (Table 4).

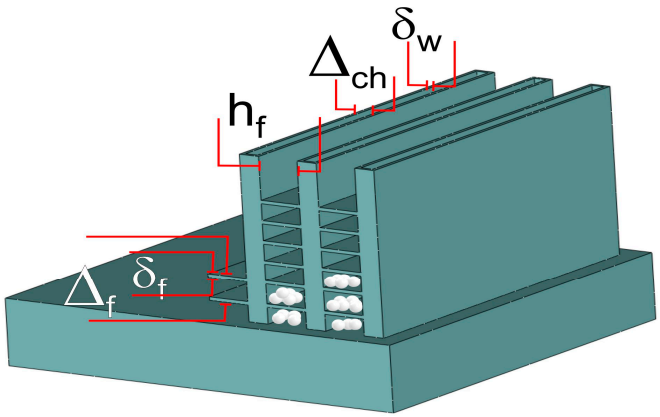

Figure 8. FFT heat exchanger dimensions.

Table 4. Characteristics considered FFT radiator.

δ_w, mm	Δ_{ch}, mm	h_f, mm	Δ_f, mm	δ_f, μm
0.5	1.0	6.2	0.8	63

With a total volume of the core of such a heat exchanger of 140 cm^3, the free volume available for loading the adsorbent is 97 cm^3. In this case, the amount of sorbent in the heat exchanger will be as high as 97 cm^3 × 0.59 g/cm^3 = 57 g. It is important to note that the sorbent will exchange about 0.1 g of water per gram of sorbent even at such extremely hot climate conditions.

4.2. Dehumidification

The air drying process takes place in an open system. Humid air enters the reactor filled with dry sorbent (Figure 9). The sorbent adsorbs vapours and provides air drying down to a desired dew point. First, the sorbent becomes wet at the reactor inlet, and then the adsorption front (the boundary between wet and dry sorbent) moves towards the end of the reactor. When comparing two sorbents (Figure 9), characterized by a different sorption capacity (higher uptake value—red line) under the same conditions, the preference should be given to a material with a higher sorption capacity (sorbent 2, Figure 9a). Indeed, for a material with a higher capacity, the adsorption front will move more slowly; thus, the time between regenerations will increase (Figure 9b).

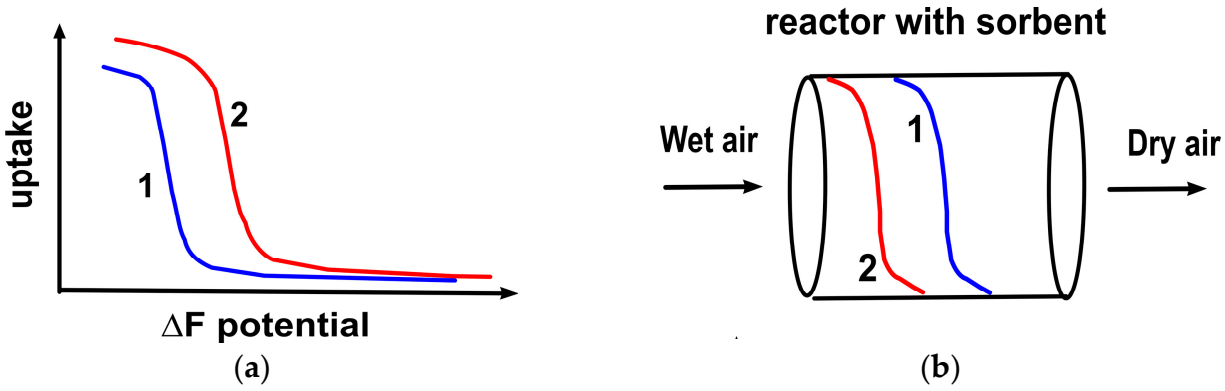

Figure 9. (**a**) Sorption curves; (**b**) profiles of humidity inside reactor for different sorbents at the same time. The first sorbent (blue), the second sorbent (red).

The standard conditions for drying compressed air were considered. Air from the environment at a temperature T_{env} = 20 °C and a humidity of 50% is compressed (pressure of water in the environment P_{env} = 12.4 mbar), as a result of which, the humidity increases to 100% (pressure of saturated water vapour $P^0(T_{env})$ = 23.3 mbar), with a regeneration temperature of 110–130 °C (T_{reg}). In order to use energy rationally, there is a need to use the lowest possible regeneration temperature. The desired dew point for laboratory compressed air is −40 °C. In this case, the Polanyi potential for regeneration can be estimated as (purple dots Figure 10):

$$\Delta F_d = -RT_{reg} \ln\left(P_{env}/P^0(T_{reg})\right) \quad (4)$$

where $P^0(T_{reg})$—saturated pressure of water at regeneration temperature T_{reg}.

On the other hand, the Polanyi potential for different dew points can be estimated (green symbols in Figure 10):

$$\Delta F_{dew\ point} = -RT_{env} \ln\left(P^0\left(T_{dew\ point}\right)/P^0(T_{env})\right), \quad (5)$$

where $P^0(T_{env})$, $P^0(T_{dew\ point})$—saturated pressure of water at temperature T_{env} and $T_{dew\ point}$, respectively.

It can be seen (Figure 10) that in the entire considered range of Polanyi potentials, the sorption capacity of the composite based on the double salt system exceeds the capacity of the composite based on pure calcium chloride ($\Delta N^*(CaCl_2 + CaBr_2\ (1{:}1))/SiO_2$), which is greater than $\Delta N^*(CaCl_2/SiO_2)$) (Figure 10). On the other hand, the composite containing

pure calcium bromide will be regenerated only at a regeneration temperature of 145 °C, while only 110 °C is sufficient for the regeneration of a composite based on a double salt system (Figure 10 ΔT_{reg}). Moreover, it is important to take into consideration the economic side of the issue—calcium chloride is a cheaper reagent than calcium bromide, so a composite based on a binary salt system will cost less than a composite based on pure calcium bromide.

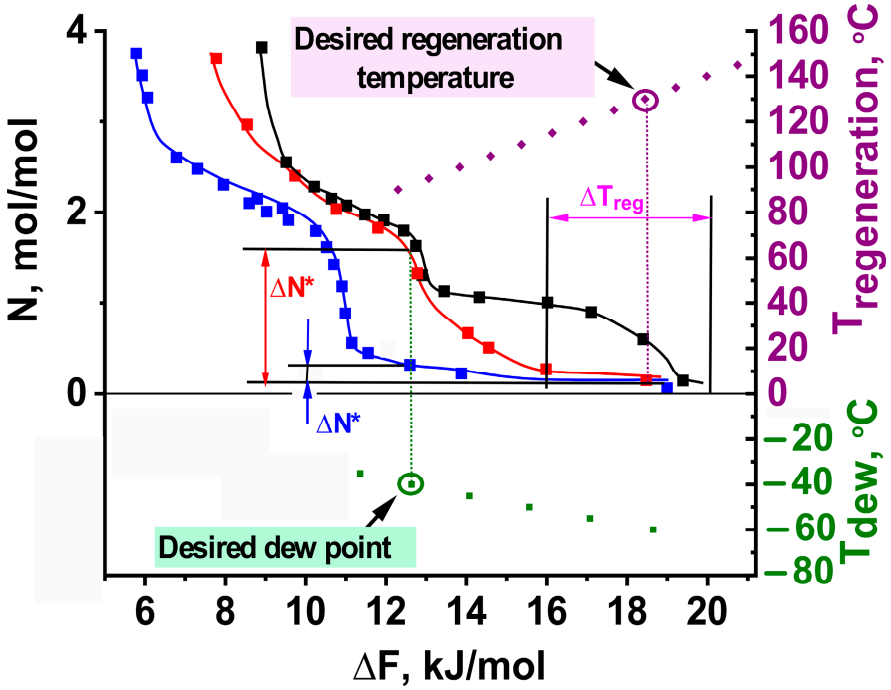

Figure 10. Dependence "N vs. ΔF" (■)—$CaCl_2/SiO_2$, (■)—($CaCl_2$ + $CaBr_2$ (1:1))/SiO_2, (■)—$CaBr_2/SiO_2$, (▪)—ΔF corresponding to different dew point values, (♦)—ΔF corresponding to different regeneration temperatures.

5. Conclusions

Using the volumetric method, the sorption equilibrium of composite sorbents based on calcium halides with water vapours is studied. The novelty of this work is the consideration of the problem of the target-oriented synthesis of sorbents with predetermined sorption properties for specific practical applications due to the formation of a $CaCl_2$-$CaBr_2$ solid solution in the pores of the silica gel. It has been shown that the presence of a solid solution of $CaCl_2$-$CaBr_2$ in matrix pores results in a change in the formation conditions of the binary salt system complex with water in comparison with the same conditions for the composites on the base of individual salts. The higher the $CaBr_2$ molar content in the composite, the lower the equilibrium pressure P* of the complex $CaCl_xBr_{2-x}\cdot NH_2O$ (N = 1, 2, 4) formation. For the composite ($CaCl_2$ + $CaBr_2$ (1:1))/SiO_2, the isosteric enthalpy and entropy of water ($\Delta H = -48 \pm 3$ kJ/mol $\Delta S = -108 \pm 2$ J/(mol·K)) sorption at uptake N = 3.6 mole/mole are midway between the same parameters for the composites on the base of pure salts $CaCl_2$ and $CaBr_2$. For the example of air conditioning in a hot climate and air drying, it is shown that by varying the molar ratio of salts inside matrix pores, it is possible to design sorption materials with optimal properties that perfectly fit the demands of particular adsorption applications. Thus, the use of the binary $CaCl_2$ + $CaBr_2$ system confined to the silica pores can be an effective tool for designing innovative materials with predetermined sorption properties.

Author Contributions: Conceptualization, A.G. and M.T.; methodology, M.T.; validation, M.S. and M.T.; formal analysis, A.C.; investigation, A.C. and M.S.; resources, A.G.; data curation, A.G. and M.T.; writing—original draft preparation, A.G.; writing—review and editing, M.T.; supervision, A.G.; project administration, A.G.; funding acquisition, A.G. All authors have read and agreed to the published version of the manuscript.

Funding: This work was supported by the Russian Science Foundation project 21-79-10183.

Data Availability Statement: Data can be provided upon request.

Conflicts of Interest: The authors declare no conflict of interest.

References

1. Dabrowski, A. Adsorption—From Theory to Practice. *Adv. Colloid Interface Sci.* **2001**, *93*, 135–224. [CrossRef] [PubMed]
2. San, J.-Y.; Lin, W.M. Comparison among three adsorption pairs for using as the working substances in a multi-bed adsorption heat pump. *Appl. Therm. Eng.* **2008**, *28*, 988–997. [CrossRef]
3. Gordeeva, L.G.; Aristov, Y.I. Adsorptive heat storage and amplification: New cycles and adsorbents. *Energy* **2019**, *167*, 440–453. [CrossRef]
4. Aristov, Y.I. Novel materials for adsorptive heat pumping and storage: Screening and nanotailoring of sorption properties. *J. Chem. Eng. Jpn.* **2007**, *40*, 1242–1251. [CrossRef]
5. Polanyi, M. Section III.—Theories of the adsorption of gases. A general survey and some additional remarks. Introductory paper to section III. *Trans. Faraday Soc.* **1932**, *28*, 316–333. [CrossRef]
6. Pons, M.; Meunier, F.; Cacciola, G.; Critoph, R.E.; Groll, M.; Puigjaner, L.; Spinner, B.; Ziegler, F. Thermodynamic based comparison of sorption systems for cooling and heat pumping. *Int. J. Refrig.* **1999**, *22*, 5–17. [CrossRef]
7. Critoph, R.E.; Zhong, Y. Review of trends in solid sorption refrigeration and heat pumping technology. *Proc. Inst. Mech. Eng. Part E J. Process Mech. Eng.* **2005**, *219*, 285–300. [CrossRef]
8. Wang, D.C.; Li, Y.H.; Li, D.; Xia, Y.Z.; Zhang, J.P. A review on adsorption refrigeration technology and adsorption deterioration in physical adsorption systems. *Renew. Sustain. Energy Rev.* **2010**, *14*, 344–353. [CrossRef]
9. Aristov, Y.I. Challenging offers of material science for adsorption heat transformation. *Appl. Therm. Eng.* **2013**, *50*, 1610–1618. [CrossRef]
10. Rahmadiawan, D.; Abral, H.; Railis, R.M.; Iby, I.C.; Mahardika, M.; Handayani, D.; Natrana, K.D.; Juliadmi, D.; Akbar, F. The Enhanced Moisture Absorption and Tensile Strength of PVA/Uncaria gambir Extract by Boric Acid as a Highly Moisture-Resistant, Anti-UV, and Strong Film for Food Packaging Applications. *J. Compos. Sci.* **2022**, *6*, 337. [CrossRef]
11. Rahmadiawan, D.; Abral, H.; Kotodeli, R.A.; Sugiarti, E.; Muslimin, A.N.; Admi, R.I.; Arafat, A.; Kim, H.-J.; Sapuan, S.M.; Kosasih, E.A. A Novel Highly Conductive, Transparent, and Strong Pure-Cellulose Film from TEMPO-Oxidized Bacterial Cellulose by Increasing Sonication Power. *Polymers* **2023**, *15*, 643. [CrossRef] [PubMed]
12. Nordin, A.H.; Norfarhana, A.S.; Noor, S.F.M.; Paiman, S.H.; Nordin, M.L.; Husna, S.M.N.; Ilyas, R.A.; Ngadi, N.; Bakar, A.A.; Ahmad, Z.; et al. Recent Advances in Using Adsorbent Derived from Agricultural Waste for Antibiotics and Non-Steroidal Anti-Inflammatory Wastewater Treatment: A Review. *Separations* **2023**, *10*, 300. [CrossRef]
13. Wang, M.; Phillips, T.D. Green-Engineered Barrier Creams with Montmorillonite-Chlorophyll Clays as Adsorbents for Benzene, Toluene, and Xylene. *Separations* **2023**, *10*, 237. [CrossRef]
14. Rodinkov, O.; Postnov, V.; Spivakovskyi, V.; Vlasov, A.; Bugaichenko, A.; Slastina, S.; Znamenskaya, E.; Shilov, R.; Lanin, S.; Nesterenko, P. Comparison of Adsorbents Containing Carbon Nanotubes for Express Pre-Concentration of Volatile Organic Compounds from the Air Flow. *Separations* **2021**, *8*, 50. [CrossRef]
15. Guo, Y.; Zhang, X.; Xie, Y.; Hu, Y.; Jia, Z.; Ma, Y.; Wang, X. Facile Separation of Cu^{2+} from Water by Novel Sandwich NaY Zeolite Adsorptive Membrane. *Separations* **2023**, *10*, 171. [CrossRef]
16. Singh, V.; Pant, N.; Sharma, R.K.; Padalia, D.; Rawat, P.S.; Goswami, R.; Singh, P.; Kumar, A.; Bhandari, P.; Tabish, A.; et al. Adsorption Studies of Pb(II) and Cd(II) Heavy Metal Ions from Aqueous Solutions Using a Magnetic Biochar Composite Material. *Separations* **2023**, *10*, 389. [CrossRef]
17. Nguyen, M.H.; Zbair, M.; Dutournié, P.; Gervasini, A.; Vaulot, C.; Bennici, S. Toward new low-temperature thermochemical heat storage materials: Investigation of hydration/dehydration behaviors of $MgSO_4$/Hydroxyapatite composite. *Sol. Energy Mater. Sol. Cells* **2022**, *240*, 111696. [CrossRef]
18. Zhou, H.; Zhang, D. Investigation on pH/temperature-manipulated hydrothermally reduced graphene oxide aerogel impregnated with $MgCl_2$ hydrates for low-temperature thermochemical heat storage. *Sol. Energy Mater. Sol. Cells* **2022**, *241*, 111740. [CrossRef]
19. Jiang, L.; Lin, Y.C.; Liu, W.; Ma, Z.W.; Wang, R.Q.; Zhang, X.J.; Roskilly, A.P. Thermophysical characterization of magnesium chloride and its application in open sorption thermal energy storage system. *Sol. Energy Mater. Sol. Cells* **2022**, *236*, 111528. [CrossRef]
20. Gordeeva, L.G.; Glaznev, I.S.; Savchenko, E.V.; Malakhov, V.V.; Aristov, Y.I. Impact of phase composition on water adsorption on inorganic hybrids "salt/silica". *J. Colloid Interface Sci.* **2006**, *301*, 685–691. [CrossRef]

21. Gordeeva, L.; Restuccia, G.; Freni, A.; Aristov, Y.I. Water sorption on composites "LiBr in a porous carbon". *Fuel Process. Technol.* **2002**, *79*, 225–231. [CrossRef]
22. Mrowiec-Białoń, J.; Lachowski, A.I.; Jarzębski, A.B.; Gordeeva, L.G.; Aristov, Y.I. SiO_2–LiBr Nanocomposite Sol–Gel Adsorbents of Water Vapor: Preparation and Properties. *J. Colloid Interface Sci.* **1999**, *218*, 500–503. [CrossRef] [PubMed]
23. Gordeeva, L.G.; Freni, A.; Krieger, T.A.; Restuccia, G.; Aristov, Y.I. Composites "lithium halides in silica gel pores": Methanol sorption equilibrium. *Microporous Mesoporous Mater.* **2008**, *112*, 254–261. [CrossRef]
24. Simonova, I.A.; Freni, A.; Restuccia, G.; Aristov, Y.I. Water sorption on composite "silica modified by calcium nitrate". *Microporous Mesoporous Mater.* **2009**, *122*, 223–228. [CrossRef]
25. Wei, S.; Zhou, W.; Han, R.; Gao, J.; Zhao, G.; Qin, Y.; Wang, C. Influence of minerals with different porous structures on thermochemical heat storage performance of $CaCl_2$-based composite sorbents. *Sol. Energy Mater. Sol. Cells* **2022**, *243*, 111769. [CrossRef]
26. Chen, Z.; Zhang, Y.; Zhang, Y.; Su, Y.; Riffat, S. A study on vermiculite-based salt mixture composite materials for low-grade thermochemical adsorption heat storage. *Energy* **2023**, *278*, 127986. [CrossRef]
27. Posern, K.; Kaps, C. Calorimetric studies of thermochemical heat storage materials based on mixtures of $MgSO_4$ and $MgCl_2$. *Thermochim. Acta* **2010**, *502*, 73–76. [CrossRef]
28. Jiang, L.; Zhu, F.Q.; Wang, L.W.; Liu, C.Z.; Wang, R.Z. Experimental investigation on a $MnCl_2$-$CaCl_2$-NH_3 thermal energy storage system. *Renew. Energy* **2016**, *91*, 130–136. [CrossRef]
29. Zhang, Y.; Wang, R. Sorption Thermal Energy Storage: Concept, Process, Applications and Perspectives. *Energy Storage Mater.* **2020**, *27*, 352–369. [CrossRef]
30. Vegard, L. Die Konstitution der Mischkristalle und die Raumfüllung der Atome. *Z. Für Phys.* **1921**, *5*, 17–26. [CrossRef]
31. Feilchenfeld, H.; Fuchs, J.; Kahana, F.; Sarig, S. The melting point adjustment of calcium chloride hexahydrate by addition of potassium chloride or calcium bromide hexahydrate. *Solar Energy* **1985**, *34*, 199–201. [CrossRef]
32. Ghosh, S.; Sridharan, R.; Gnanasekaran, T. Studies on the phase diagram of $CaCl_2$–$CaBr_2$ system. *Thermochim. Acta* **2010**, *505*, 69–72. [CrossRef]
33. Liu, C.Y.; Aika, K.-I. Ammonia absorption into alkiline earth metal halide mixtures as an ammonia storage material. *Ind. Eng. Chem. Res.* **2004**, *43*, 7484–7491. [CrossRef]
34. Liu, C.Y.; Aika, K.-I. Effect of the Cl/Br ratio of a $CaCl_2$–$CaBr_2$ mixture used as an ammonia storage material. *Ind. Eng. Chem. Res.* **2004**, *43*, 6494–7000. [CrossRef]
35. Gordeeva, L.; Grekova, A.; Krieger, T.; Aristov, Y. Composites "binary salts in porous matrix" for adsorption heat transformation. *Appl. Therm. Eng.* **2013**, *50*, 1633–1638. [CrossRef]
36. Grekova, A.D.; Veselovskaya, J.V.; Tokarev, M.M.; Krieger, T.A.; Shmakov, A.N.; Gordeeva, L.G. Ammonia sorption on the composites "($BaCl_2$+$BaBr_2$) inside vermiculite pores". *Colloids Surf. A Physicochem. Eng. Asp.* **2014**, *448*, 169–174. [CrossRef]
37. Veselovskaya, J.V.; Tokarev, M.M.; Grekova, A.D.; Gordeeva, L.G. Novel ammonia sorbents "porous matrix modified by active salt" for adsorptive heat transformation: 6. The ways of adsorption dynamics enhancement. *Appl. Therm. Eng.* **2012**, *37*, 87–94. [CrossRef]
38. Grekova, A.D.; Veselovskaya, J.V.; Tokarev, M.M.; Gordeeva, L.G. Novel ammonia sorbents "porous matrix modified by active salt" for adsorptive heat transformation: 5. Designing the composite adsorbent for ice makers. *Appl. Therm. Eng.* **2012**, *37*, 80–86. [CrossRef]
39. Gordeeva, L.G.; Grekova, A.D.; Krieger, T.A.; Aristov, Y.I. Adsorption properties of composite materials (LiCl + LiBr)/silica. *Microporous Mesoporous Mater.* **2009**, *126*, 262–267. [CrossRef]
40. Bülow, M.; Shen, D.; Jale, S. Measurement of sorption equilibria under isosteric conditions: The principles, advantages and limitations. *Appl. Surf. Sci.* **2002**, *196*, 157–172. [CrossRef]
41. Yanagi, H.; Okamoto, N.; Komatsu, F.; Ino, N.; Ogura, M.; Nishino, M.; Okamoto, Y. Development of Adsorption Refrigerator using Silicagel-Water Pairs. In *Studies in Surface Science and Catalysis*; Suzuki, M., Ed.; Elsevier: Amsterdam, The Netherlands, 1993; Volume 80, pp. 751–758. [CrossRef]
42. Aristov, Y.I.; Gordeeva, L.G. Combining the psychrometric chart of humid air with water adsorption isosters: Analysis of the Ventireg process. *Energy* **2022**, *239*, 122278. [CrossRef]
43. Glaznev, I.S.; Aristov, Y.I. The effect of cycle boundary conditions and adsorbent grain size on the water sorption dynamics in adsorption chillers. *Int. J. Heat Mass Transf.* **2010**, *53*, 1893–1898. [CrossRef]
44. Aristov, Y.I.; Tokarev, M.M.; Cacciola, G.; Restuccia, G. Selective water sorbents for multiple applications: 1. $CaCl_2$ confined in mesopores of the silica gel: Sorption properties. *React. Kinet. Catal. Lett.* **1996**, *59*, 325–334. [CrossRef]
45. Sapienza, A.; Glaznev, I.S.; Santamaria, S.; Freni, A.; Aristov, Y.I. Adsorption chilling driven by low temperature heat: New adsorbent and cycle optimization. *Appl. Therm. Eng.* **2012**, *32*, 141–146. [CrossRef]
46. Freni, A.; Russo, F.; Vasta, S.; Tokarev, M.; Aristov, Y.I.; Restuccia, G. An advanced solid sorption chiller using SWS-1L. *Appl. Therm. Eng.* **2007**, *27*, 2200–2204. [CrossRef]
47. Almohammadi, K.M.; Harby, K. Operational conditions optimization of a proposed solar-powered adsorption cooling system: Experimental, modeling, and optimization algorithm techniques. *Energy* **2020**, *206*, 118007. [CrossRef]
48. Chen, Q.F.; Du, S.W.; Yuan, Z.X.; Sun, T.B.; Li, Y.X. Experimental study on performance change with time of solar adsorption refrigeration system. *Appl. Therm. Eng.* **2018**, *138*, 386–393. [CrossRef]

49. Liu, Y.M.; Yuan, Z.X.; Wen, X.; Du, C.X. Evaluation on performance of solar adsorption cooling of silica gel and SAPO-34 zeolite. *Appl. Therm. Eng.* **2021**, *182*, 116019. [CrossRef]
50. Tso, C.Y.; Chan, K.C.; Chao, C.Y.H.; Wu, C.L. Experimental performance analysis on an adsorption cooling system using zeolite 13X/$CaCl_2$ adsorbent with various operation sequences. *Int. J. Heat Mass Transf.* **2015**, *85*, 343–355. [CrossRef]
51. Roumpedakis, T.C.; Vasta, S.; Sapienza, A.; Kallis, G.; Karellas, S.; Wittstadt, U.; Tanne, M.; Harborth, N.; Sonnenfeld, U. Performance Results of a Solar Adsorption Cooling and Heating Unit. *Energies* **2020**, *13*, 1630. [CrossRef]
52. Mohammed, R.H.; Mesalhy, O.; Elsayed, M.L.; Chow, L.C. Performance evaluation of a new modular packed bed for adsorption cooling systems. *Appl. Therm. Eng.* **2018**, *136*, 293–300. [CrossRef]
53. Chan, K.C.; Tso, C.Y.; Wu, C.; Chao, C.Y.H. Enhancing the performance of a zeolite 13X/$CaCl_2$–water adsorption cooling system by improving adsorber design and operation sequence. *Energy Build.* **2018**, *158*, 1368–1378. [CrossRef]
54. Wang, R.Z. Performance improvement of adsorption cooling by heat and mass recovery operation. *Int. J. of Refrig.* **2001**, *24*, 602–611. [CrossRef]
55. Grekova, A.; Tokarev, M. An Optimal Plate Fin Heat Exchanger for Adsorption Chilling: Theoretical Consideration. *Int. J. Thermofluids* **2022**, *16*, 100221. [CrossRef]
56. Grekova, A.; Krivosheeva, I.; Solovyeva, M.; Tokarev, M. Express Method for Assessing Optimality of Industrial Heat Exchangers for Adsorption Heat Transformation. *Fluids* **2023**, *8*, 14. [CrossRef]